

Relative contributions to the plasmon line shape of metal nanoshellsS. L. Westcott,¹ J. B. Jackson,² C. Radloff,³ and N. J. Halas^{1,3,*}¹*Department of Electrical and Computer Engineering, MS-366, Rice University, P.O. Box 1892, Houston, Texas 77251-1892*²*Department of Physics and Astronomy, MS-61, Rice University, P.O. Box 1892, Houston, Texas 77251-1892*³*Department of Chemistry, MS-60, Rice University, P.O. Box 1892, Houston, Texas 77251-1892*

(Received 14 November 2001; revised manuscript received 29 January 2002; published 31 October 2002)

Nanoshells are mesoscopic particles consisting of a dielectric core coated with a metal shell, in particular gold or silver, of uniform nanometer scale thickness. This topology supports plasmon excitations with frequencies that are sensitively dependent on the relative radii of the nanoparticle's core and shell. The plasmon linewidth for this geometry is typically quite broad, nominally 100 nm or more in wavelength at plasmon resonance wavelengths in the near infrared. Several distinct physical mechanisms control the plasmon line-shape: phase retardation effects, including multipolar plasmon contributions; inhomogeneous broadening due to core and shell size distributions; and electron scattering at the shell interfaces. These mechanisms are examined in terms of their relative contributions to the plasmon line shape for nanoshells fabricated with diameters of 100–250 nm.

DOI: 10.1103/PhysRevB.66.155431

PACS number(s): 78.67.Bf, 73.22.Lp, 78.40.Kc

I. INTRODUCTION

For conduction electrons in a metal, the confining forces on the electrons at interfaces result in resonant frequencies for electron motion known as plasmon resonances. When the electrons are driven by an electromagnetic wave near the plasmon resonance frequency, the optical response is enhanced, causing greater absorption and scattering of the light and inducing large fields near the metal's surface. For mesoscopic metals, such as colloidal nanospheres, nanorods or nanoshells, the properties of the plasmon resonance are controlled by the dielectric function of the constituent metal and the embedding medium, and also by the shape of the nanostructure.¹ For nanoscale topologies such as nanoshells or nanorods, the various properties of the plasmon resonance, such as its frequency and line shape, become a highly sensitive function of the precise mesoscopic topology of the nanostructure: for nanorods, the aspect ratio largely determines the plasmon resonances;² for nanoshells, the core/shell ratio is largely responsible for the plasmon resonance frequency supported by this geometry.^{3–5}

In this paper, we describe the important characteristics of the nanoshell plasmon resonance and how the core-shell geometry determines those properties. We address the physical mechanisms that contribute to the line shape of the plasmon resonance for isolated nanoshells, as a function of relative and absolute core and shell dimensions. We also delineate the relative contributions of inhomogeneous effects, such as variations in core and shell dimensions, from homogeneous contributions to the line shape, for nanoshell dimensions that are currently straightforward to fabricate.

II. NANOSHELL FABRICATION

The basic geometry of a nanoshell, a dielectric core coated with a thin metal shell, is shown in Fig. 1. There are two reliable methods for synthesizing metallic nanoshells (1) a one-step chemical method and (2) a sequential deposition of a shell layer onto a previously synthesized dielectric nano-

particle core. The first method involves the chemical reduction of HAuCl_4 to Au in the presence of an aged Na_2S solution.⁶ This reaction results in both solid gold nanoparticles and nanoparticles with a gold sulfide core and gold shell. The dimensions of the nanoshells can be controlled over a narrow range by adjusting the reactant ratio, resulting in nanoshells with plasmon resonances that can be varied over a nominal 300 nm wavelength range. The growth kinetics of Au_2S -Au nanoshell formation,⁷ the linear optical properties of the nanoshells produced by this synthetic method,^{7,8} and the ultrafast electron dynamics in the mesoscopic shell layer,^{9,10} including the effect of adsorbed molecules on the electron thermalization dynamics in the shell layer,¹¹ have been studied.

The second, sequential deposition method permits independent control over the sizes of the constituent core and shell of the nanoparticles as well as their chemical composition.^{5,12} Silica nanoparticles with polydispersity of less than 10% are used as the nanoparticle cores. Ultrasmall gold nanoparticles (≤ 2 nm diameter) are then chemically attached (usually via a linking molecule such as aminopropyltrimethoxysilane) to the surface of the silica nanoparticles. A solution of potassium carbonate and HAuCl_4 is then mixed with the silica nanoparticles. Using formaldehyde, the HAuCl_4 is reduced and preferentially deposited onto the bound gold nanoparticles. During this deposition step, the

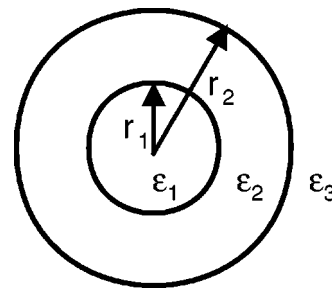


FIG. 1. A nanoshell of total radius r_2 consists of a dielectric core of radius r_1 and a metal shell of thickness $r_2 - r_1$.

bound gold nanoparticles increase in size and coalesce into a gold shell of uniform nanometer scale thickness. The final thickness is controlled by the reactant concentrations. The small fraction of solid gold nanoparticles that are formed as a side product are easily removed by centrifugation. This multistep synthesis has recently been modified for the fabrication of silica-silver nanoshells.¹³

The extinction spectra of the nanoshells reported here are determined by combining measurements taken on a Hitachi U-2001 UV-visible spectrophotometer (400 to 1050 nm range) with those taken in the near infrared (700 to 1400 nm) using a Nicolet Magna-IR 560 spectrometer. With both instruments, cuvettes filled with water were used as a reference. The experimental spectra were spliced at 825 nm with good agreement throughout the overlapped range. Transmission electron microscope (TEM) images of the silica core nanoparticles and the nanoshells were obtained on a JEOL-2010 TEM operating at 100 kV and used to determine particle size, polydispersity, and the degree of aggregation.

III. OPTICAL PROPERTIES

In an optical field, a nanoparticle much smaller than the wavelength of light will respond as a dipole. In this dipole limit, the absorption and scattering cross sections of both solid nanoparticles and nanoshells can be analytically obtained.^{3,4} In the dipole approximation for given core, shell, and embedding media, the wavelength at which the plasmon resonance occurs depends only on the ratio of the total radius to the core radius, r_2/r_1 , and not the absolute sizes. As the nanoparticle size increases to be comparable to the wavelength of light, higher order multipolar contributions to the overall optical response can be excited due to the spatial variation of the electromagnetic field across the breadth of the nanostructure.¹⁴ Mie scattering theory expresses the time-varying electric fields in and near the nanoparticle in terms of a set of vector basis functions chosen so that each term in the expansion corresponds to one of the resonance modes.^{3,15} Matching the boundary conditions for the electric and magnetic fields at the interfaces between the core/shell and the shell/medium determines the scattering, absorption and extinction cross sections of the particles, the angular distribution of the scattered light,¹⁴ and the field intensities in and around the particle.

The coherence lifetime of the dipole plasmon resonance in solid metal nanoparticles is ≤ 20 fs,¹⁶ therefore this resonance possesses an inherently broad linewidth.¹⁷ The three major factors expected to contribute to the observed linewidth of the nanoshell plasmon resonance are (1) phase retardation effects, (2) the finite size distribution of core-shell nanoparticles, resulting in an inhomogeneous contribution to the plasmon linewidth for an ensemble of nanoshells, and (3) electron-interface scattering within the shell layer. These factors can be explained using classical electromagnetic theory. Quantum confinement (i.e., the splitting of the conduction band into discrete levels) is not required to explain the plasmon linewidth. We examine, both theoretically and by comparing our calculations to experimental spectra, the relative contributions of these three effects to the plasmon linewidth

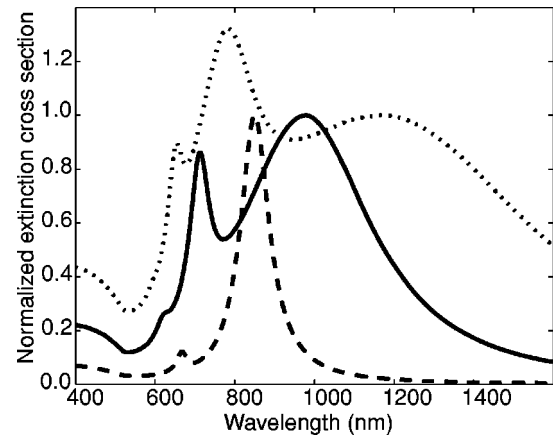


FIG. 2. Theoretical extinction cross sections of nanoshells in water with a silica core and gold shell of 45 nm radius and 5.7 nm thickness (dashed), 91.5 nm radius and 11.5 nm thickness (solid), and 135 nm radius and 17 nm thickness (dotted). The cross sections have been normalized to have the same magnitudes at the dipole resonances.

for silica core-gold shell nanoparticles in a readily accessible size range.

A. Phase retardation effects

As a gold nanoshell is scaled larger in size from the dipole limit, its plasmon linewidth is broadened dramatically. This is illustrated in Fig. 2. In this figure, extinction cross sections calculated for silica-gold nanoshells with the r_2/r_1 ratio of 1.13 are shown. The cross sections are calculated using the measured dielectric function of an evaporated film of gold¹⁸ as the dielectric function of the gold shell. In the dipole approximation, the wavelength at which the resonance occurs would remain constant as the total particle size is increased. However, using full Mie scattering theory, the wavelength at which the resonance occurs for a given r_2/r_1 ratio increases with the absolute nanoparticle size. In addition, the full width at half maximum (FWHM) which is only 90 nm for the smallest nanoshell (101.4 nm diameter) increases dramatically to 945 nm for the largest nanoshell shown (304 nm diameter). The shift in resonance and increase in linewidth are due solely to the phase retardation of the electric field that occurs as the size of the nanoshells becomes comparable to the wavelength of the light.¹ This phase retardation is also responsible for the excitation of spectrally distinct higher order plasmon modes, such as the quadrupole plasmon peak feature seen here in the 600–800 nm range.¹⁴ Even though the plasmon modes remain spectrally separated in nanoshells, all the resonances broaden with increasing particle size.

In Fig. 2 the extinction cross sections are normalized to allow comparison of the dipole plasmon linewidths. The integrated extinction spectrum scales as the cross sectional area of the nanoshell just as for solid metal nanoparticles, in accordance with energy conservation.

B. Core and shell size distribution

Statistical variations in particle size are experimentally inevitable for both the core and shell layers of a nanoshell.

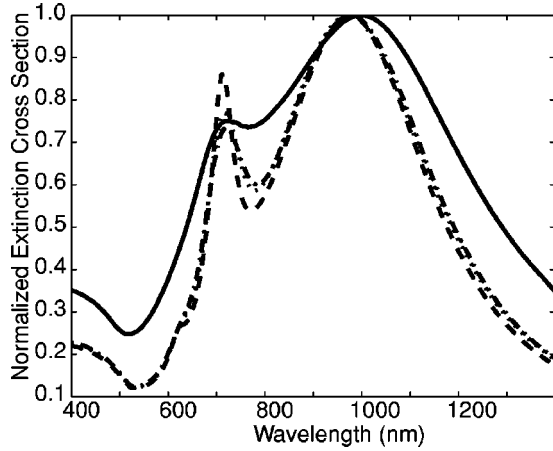


FIG. 3. Measured extinction (solid line) with normalized extinction cross sections calculated from the measured dielectric function of gold (Ref. 18) with no size distribution (dashed), a 7% core radius distribution (dotted), or a 7% core radius distribution and 10% shell thickness distribution (dash-dot). Dimensions are 91.5 nm core radius and 103 nm total radius.

To examine the relative contribution to the plasmon linewidth of such size distributions we incorporate the observed size variations as Gaussian distributions in our Mie scattering theory calculations. To include a core distribution, extinction cross sections for 50 different core sizes ranging from two standard deviations below the average core size to two standard deviations above are calculated. These extinction cross sections are weighted by the magnitude of the Gaussian distribution and summed. A similar procedure is followed for a Gaussian shell size distribution. To include both distributions, the procedure is repeated twice, necessitating a total of 2500 different cross sections in the sum.

In Fig. 3, the solid line is the measured extinction¹⁹ of a solution of nanoshells. Since the volume fraction of nanoshells in the solution was only 7×10^{-5} , the measured extinction of the nanoshell solution should be proportional to the extinction cross section of a single nanoshell, the concentration of nanoshells, and the optical pathlength.¹ From TEM images, the core nanoparticles were determined to have a radius of 86 ± 6 nm, while the complete nanoshells had a radius of 102 ± 4 nm. The dashed line is the extinction cross section for a gold nanoshell with a 91.5 nm silica core radius and a 11.5 nm thick gold shell calculated using the measured dielectric function of gold.¹⁸ The size of the silica core observed in TEM images is frequently 5 to 10% less than the size determined from the best fit to the nanoshell extinction due to the shrinking of the porous silica nanoparticles when exposed to the electron beam of the TEM.²⁰ The experimental linewidth is much broader than that calculated from the measured dielectric function of gold.¹⁸ The dotted line is the extinction cross section calculated incorporating a core size distribution of 7%, as was determined by TEM. The dot-dash line is the extinction cross section which incorporates a core size distribution of 7% and a shell size distribution of 10%. This shell size distribution is probably larger than the physical size distribution given that the distribution of particle sizes decreases for the complete nanoshells compared to the

core nanoparticles. Despite that, the extinction cross section is still not as broad as the experimental linewidth: this discrepancy is due to electron-interface scattering as described in the next section.

C. Electron-interface scattering

Electron-interface scattering is a broadening mechanism introduced by electron scattering in the thin shell and is evidence of a deviation of the gold in the shell layer from its bulk dielectric properties. The dielectric function $\epsilon(\omega)$ of gold can be modeled as having two components: the first due to *d*-band to conduction band electron transitions $\epsilon(\omega)_{\text{interband}}$ and the second due to Drude conduction electrons:

$$\epsilon(\omega) = \epsilon(\omega)_{\text{interband}} + \left(1 - \frac{\omega_p^2}{\omega^2 + i\omega\gamma_{\text{bulk}}} \right) \quad (1)$$

where ω is the frequency, ω_p is the bulk plasma frequency (1.37×10^{16} rad s^{-1}) and γ_{bulk} is the bulk collision frequency (3.33×10^{13} s^{-1}).²¹ The bulk collision frequency embodies a number of physical processes such as electron-electron, electron-phonon, and electron-impurity interactions. However, in the case of mesoscopic metal structures, when one dimension of the metal is reduced below the electron mean free path, an additional collision frequency, corresponding to electron-interface scattering at the inner and outer interfaces of the metal layer, becomes significant.¹ In the case of gold, the electron mean free path at room temperature is ~ 42 nm. To accommodate the reduced mean free path of electrons due to the boundaries of the thin metallic shell, a modified collision frequency Γ is introduced into the dielectric function, with an additional electron-interface scattering term related to the thickness of the shell:

$$\Gamma = \gamma_{\text{bulk}} + Av_F/d, \quad (2)$$

where γ_{bulk} is the bulk collision frequency described above, v_F is the Fermi velocity (1.4×10^6 m s^{-1}),²¹ and d is the shell thickness. The parameter A has been used to account for the angular nature of electron scattering, the shape of nanoparticles, and the chemical interface between nanoparticle and embedding medium.¹ The modified collision frequency is incorporated into the measured dielectric values $\epsilon(\omega)_{\text{exp}}$ ¹⁸ to determine the size-dependent dielectric function of gold $\epsilon(a, \omega)$:

$$\epsilon(a, \omega) = \epsilon(\omega)_{\text{exp}} + \frac{\omega_p^2}{\omega^2 + i\omega\gamma_{\text{bulk}}} - \frac{\omega_p^2}{\omega^2 + i\omega\Gamma}. \quad (3)$$

In Fig. 4(a), the effects of increased electron-interface scattering are demonstrated for the same nanoshells as described in Fig. 3. The dotted line is the extinction spectrum calculated using $A=3$. The extinction spectrum calculated with the inclusion of electron-interface scattering (dotted line) does a good job of reproducing the linewidth of the measured spectrum (solid line).

In Fig. 4(b), the measured extinction of nanoshells grown with a thicker shell on the same silica core nanoparticles is

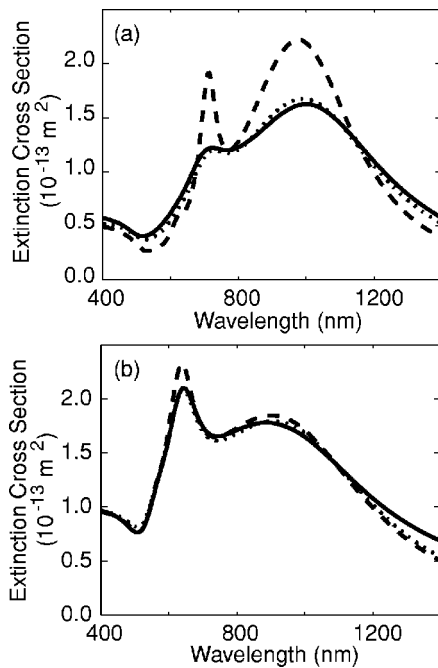


FIG. 4. Measured extinction (solid lines) scaled to the extinction cross section calculated from the measured dielectric function of gold (Ref. 18) (dashed) or incorporating electron scattering at the interfaces (dotted). Dimensions are (a) 91.5 nm core radius and 103 nm total radius and (b) 91.5 nm core radius and 115 nm total radius.

shown as a solid line. For these nanoshells with a thicker shell, the dipole plasmon shifts to shorter wavelengths, as predicted by the dipole approximation for the change in core/shell ratio.¹ The relative contribution of the quadrupole plasmon increases, as predicted for particles of larger size.¹ From TEM images, the total radius of these nanoshells was 115 ± 5 nm. The extinction cross section calculated from the measured dielectric function of gold¹⁸ is shown as a dashed line and is much closer to matching the line width of these particles with a thicker shell. However, including additional electron-interface scattering with $A = 2$, as shown in the dotted line, still provides a better match with respect to the relative heights of the quadrupole and dipole peaks. The slight discrepancy between the calculated extinction and measured extinction seen at longer wavelengths is attributed to the presence of nanoshell aggregates in the solution.¹⁴

In order to reproduce the linewidth of the measured spectra, a value of A greater than one is required. This implies that the effective path length between electron scattering events is less than the shell thickness. This may be due to the manner in which the shell grows from many nucleation points, resulting in grain boundaries and fissures near the surface when the shell coalesces. Scattering from these grain boundaries and fissures could result in shorter effective path lengths.²² As the shell is grown thicker, the surface may become smoother, leading to an increased effective path length. In comparison, for highly crystalline $\text{Au}_2\text{S-Au}$ nanoshells, a value of A equal to 1 accurately accounts for the linewidth of the plasmon resonances. For those nanoshells, the shell thickness was typically only 3 to 5 nm. For $\text{Au}_2\text{S-Au}$ nanoshells, the contribution of electron-interface scattering dominates the plasmon linewidth even with particle size distributions of 15–20%.^{7,8}

IV. CONCLUSION

In this paper we have investigated the major contributions to linewidth broadening of the plasmon resonance in a dielectric core-metal shell nanostructure. The three mechanisms that contribute to the broad spectral response of the plasmon are (1) phase retardation effects due to the finite size of the nanostructure, (2) inhomogeneous broadening due to a distribution in core and shell sizes, and (3) electron-interface scattering, which modifies the dielectric function of the shell layer and scales inversely with shell thickness. The two homogeneous broadening mechanisms of phase retardation and electron-interface scattering contribute far more to the plasmon linewidth than does the variation in particle size. The relative contributions of these three mechanisms depend both on the core/shell ratio and on the absolute size of the nanoshell constituent layers, as well as the relative size of the nanostructure compared to the wavelength of incident light at resonance.

ACKNOWLEDGMENTS

We gratefully acknowledge the contributions of Dipankar Sarkar, Richard Averitt, and Steve Oldenburg in the historical development of electromagnetic Mie scattering software over the course of this project. We thank the Robert A. Welch Foundation, the Army Research Office, and the National Science Foundation (Grant No. ECS-9801707) for support.

*Email address: halas@rice.edu

¹U. Kreibig and M. Vollmer, *Optical Properties of Metal Clusters* (Springer, Berlin, 1995).

²S. Link and M.A. El-Sayed, *J. Phys. Chem. B* **103**, 8410 (1999).

³A.L. Aden and M. Kerker, *J. Appl. Phys.* **22**, 1242 (1951).

⁴A.E. Neeves and M.H. Birnboim, *J. Opt. Soc. Am. B* **6**, 787 (1989).

⁵S.J. Oldenburg, R.D. Averitt, S.L. Westcott, and N.J. Halas, *Chem. Phys. Lett.* **288**, 243 (1998).

⁶H.S. Zhou, I. Honma, H. Komiyama, and J.W. Haus, *Phys. Rev. B* **50**, 12 052 (1994).

⁷R.D. Averitt, D. Sarkar, and N.J. Halas, *Phys. Rev. Lett.* **78**, 4217 (1997).

⁸R.D. Averitt, S.L. Westcott, and N.J. Halas, *J. Opt. Soc. Am. B* **16**, 1824 (1999).

⁹R.D. Averitt, S.L. Westcott, and N.J. Halas, *Phys. Rev. B* **58**, 10 203 (1998).

¹⁰R.D. Averitt, S.L. Westcott, and N.J. Halas, *J. Opt. Soc. Am. B* **16**, 1814 (1999).

¹¹S.L. Westcott, R.D. Averitt, J.A. Wolfgang, P. Nordlander, and N.J. Halas, *J. Phys. Chem. B* **105**, 9913 (2001).

¹²S.J. Oldenburg, J.B. Jackson, S.L. Westcott, and N.J. Halas, *Appl.*

- Phys. Lett. **75**, 2897 (1999).
- ¹³J.B. Jackson and N.J. Halas, J. Phys. Chem. B **105**, 2743 (2001).
- ¹⁴S.J. Oldenburg, G.D. Hale, J.B. Jackson, and N.J. Halas, Appl. Phys. Lett. **75**, 1063 (1999).
- ¹⁵D. Sarkar and N.J. Halas, Phys. Rev. E **56**, 1102 (1997).
- ¹⁶B. Lamprecht, J.R. Krenn, A. Leitner, and F.R. Aussenegg, Phys. Rev. Lett. **83**, 4421 (1999).
- ¹⁷T. Klar, M. Perner, S. Grosse, G. von Plessen, W. Spirkl, and J. Feldmann, Phys. Rev. Lett. **80**, 4249 (1998).
- ¹⁸P.B. Johnson and R.W. Christy, Phys. Rev. B **6**, 4370 (1972).
- ¹⁹Extinction is equal to \log_{10} (Incident Intensity/Transmitted Intensity).
- ²⁰A.P. Philipse and A. Vrij, J. Colloid Interface Sci. **128**, 121 (1989).
- ²¹N.W. Ashcroft and N.D. Mermin, Solid State Physics (W. B. Saunders, Philadelphia, 1976).
- ²²P. Mulvaney, Langmuir **12**, 788 (1996).